

# Linear and Non-linear Interdependence of EEG and HRV Frequency Bands in Human Sleep

Ramiro Chaparro-Vargas<sup>\*1</sup> *Member*, P. Chamila Dissanayaka<sup>\*2</sup>, Chanakya Reddy Patti<sup>\*3</sup>, Claudia Schilling<sup>†4</sup>, Michael Schredl<sup>†5</sup>, Dean Cvetkovic<sup>\*6</sup> *Member*

**Abstract**—The characterisation of functional interdependencies of the autonomic nervous system (ANS) stands an ever-growing interest to unveil electroencephalographic (EEG) and Heart Rate Variability (HRV) interactions. This paper presents a biosignal processing approach as a supportive computational resource in the estimation of sleep dynamics. The application of linear, non-linear methods and statistical tests upon 10 overnight polysomnographic (PSG) recordings, allowed the computation of wavelet coherence and phase locking values, in order to identify discerning features amongst the clinical healthy subjects. Our findings showed that neuronal oscillations  $\theta$ ,  $\alpha$  and  $\sigma$  interact with cardiac power bands at mid-to-high rank of coherence and phase locking, particularly during NREM sleep stages.

## I. INTRODUCTION

The bioelectrical activity of the neuronal cortex, accompanied by Heart Rate Variability (HRV) fluctuations, are two major actuators in the regulation of the sympathetic and vagal cardiac dynamics of the Autonomic Nervous System (ANS) [1]. Henceforth, the development of biosignal processing techniques over electroencephalographic (EEG) and electrocardiographic (ECG) recordings points to elucidate the characteristics of interdependencies across sleep stages. We also suggest a computational approach supported by time-frequency and phase-oriented methods to quantify the functional interactions between EEG and HRV power bands.

Until now, the research works about EEG $\leftrightarrow$ HRV interdependence have made use of linear and non-linear procedures to identify unique features during resting, task-oriented or sleeping conditions [2]. The application of analyses based on the extraction of instantaneous amplitudes, frequencies and phases has demonstrated the sporadic appearance of coupled oscillations between high-regime HRV and low-regime EEG power bands; such as HRV-HF (0.15-0.4 Hz),  $\delta$  (0.5-4 Hz),  $\theta$  (4-8 Hz) and  $\alpha$  (8-12 Hz), respectively [3] [1] [4]. However, those investigations have been mainly undertaken for either EEG $\leftrightarrow$ EEG or cardiorespiratory cross-evaluations, within electrophysiological recordings of limited duration (less than 1 hour). Subsequent studies have promoted more

sophisticated methods to estimate apart from the functional interaction, also directional interdependence, taking into account sleep stages progression [5] [6]. In this paper, the aim is to introduce linear and non-linear directed interdependencies along sleeping periods, which were observed through more extensive polysomnographic (PSG) recordings. Additional findings are pending to be clarified, regarding fast time-varying events, recurrent patterns and the corresponding interpretation of their physiological relevance.

In this paper, we propose a computational approach to perform linear, non-linear and statistical analyses over long-term PSG recordings, considering 15 EEG and 1 ECG channels. Relying on recognised methods, e.g. Wavelet Coherence and  $n:m$  phase synchronisation; we attempt to characterise the functional interdependencies of 10 healthy subjects along an overnight sleeping period. Our results suggest the presence of spectral and phase-related dependencies of neuronal and cardiac power bands with spatial divergences and constrained to sleep stages. Also, the sleep staging plays a major role in the differentiation of sympathetic and parasympathetic activity on each subject. In this sense, we encourage the adoption of biosignal processing as an assisting tool for a more precise interpretation of ANS activity during sleeping periods.

## II. METHODS

The characterisation of functional interdependence between EEG  $\leftrightarrow$  HRV power bands is composed by three main stages: pre-processing, processing and statistical analysis. The pre-processing stage strives a preliminary deployment for the raw EEG/ECG signals, including epoch segmentation, inter-neural clustering and power band decomposition [7]. Afterwards, the processing stage performs the extraction of features, appealing to Time-Frequency Analysis (TFA) and phase synchronisation techniques. The last but not least, a statistical rank test pursues significant differences within the yielded features and the previously scored sleep stages, attending to the non-linearity, non-stationarity and non-Gaussianity attributes of the original sets of data. The complete computational analysis was developed with the software package MATLAB<sup>©</sup> 7.13 (The MathWorks Inc., USA).

### A. Subjects and clinical data

The PSG recordings were obtained from 10 healthy subjects. Each subject undertook an overnight PSG recording at the Sleep Laboratory of the Central Institute of Mental Health

<sup>\*</sup> Affiliated to with School of Electrical and Computing Engineering, RMIT University, Melbourne VIC 3001, Australia

<sup>†</sup> Affiliated to clinical research physician at the sleep laboratory of the Central Institute of Mental Health, Mannheim, Germany

<sup>1</sup> E-mail: ramiro.chaparro-vargas@rmit.edu.au

<sup>2</sup> E-mail: s3304790@student.rmit.edu.au

<sup>3</sup> E-mail: s3315014@student.rmit.edu.au

<sup>4</sup> E-mail: claudia.schilling@zi-mannheim.de

<sup>5</sup> E-mail: michael.schredl@zi-mannheim.de

<sup>6</sup> E-mail: dean.cvetkovic@rmit.edu.au

in Mannheim, Germany. In accordance to the Rechtschaffen and Kales (R&K) scoring manual, EEG signals are partitioned into 30-second epochs to categorise the overall sleep staging with Wake (W), Stage 1 (S1), Stage 2 (S2), Stage 3 (S3) and Stage 4 (S4) and Rapid Eye Movement (REM) sleep categories. The study was approved by the local ethic committee of the Medical Faculty Mannheim of the University of Heidelberg, Germany.

### B. Pre-processing

Initially, the pre-processing routine performs a partition of consecutive 30-second epochs per PSG channel, intending to conserve power and time alignment properties. Next, inter-neural clustering associates EEG signals into a single composite, based on correlation coefficients and distribution divergence measures amongst nearby electrodes. For instance,  $C_{4:3}$  merges three different sources, whereas central (Cz), right- (C4) and left hemisphere (C3) locations of the scalp, plot statistically resemblant potentials in an inter-hemispheric context [6]. By averaging out the correlated EEG monopolar channels (bipolar electrodes are excluded for compatibility reasons), the clustering routine groups the inter-neural areas [8] as Table I depicts.

At the end, the power bands decomposition routine deconstructs the inter-neural clusters into 6 oscillatory bands, such as delta  $\delta$  (0.5-4 Hz), theta  $\theta$  (4-8 Hz), alpha  $\alpha$  (8-12 Hz), sigma  $\sigma$  (12-16 Hz), beta  $\beta$  (16-32 Hz) and gamma  $\gamma$  (32-64 Hz). Similarly, HRV frequency bands LF (0.04-0.15 Hz) and HF (0.15-0.4 Hz) [9] [2] are computed from the ECG signal by using R-to-R interval (RRI) computation, an algorithm for sequential peak detection, smoothing by interpolation and a final upsampling step, just as the guidelines in [9] consign. Here, the introduction of Wavelet Packet Transform (WPT) allows a time-frequency decomposition supported on the coefficients shrinkage principle to generate the aforementioned EEG and HRV frequency bands [10].

### C. Processing

The processing stage deals with the features extraction task, in an attempt to characterise the functional interdependencies between neuronal and cardiac power activity amongst the decomposed frequency bands [5] [1]. Previously, linear measures have demonstrated their suitability to estimate synchronisation tendencies, in this case, we employed coherence supported by the continuous wavelet transform (CWT) for its computation [8]. Wavelet coherence computes the auto-

and cross-power spectrum  $\mathbf{S}(\cdot)$  to produce an unitary value, matching time translation and frequency scale domains.

$$\kappa_{xy}^2(\omega_0) = \frac{|\mathbf{S}(\mathbf{W}_{xx}^H(s, \tau)\mathbf{W}_{yy}(s, \tau))|^2}{|\mathbf{S}(\mathbf{W}_{xx}(s, \tau))||\mathbf{S}(\mathbf{W}_{yy}(s, \tau))|} \quad (1)$$

where  $\mathbf{W}(s, \tau)$  denotes the continuous wavelet transform at scale  $s$  and translation index  $\tau$ .

For the present paper, we designate  $n:m$  phase synchronisation as the preferred approach for non-linear estimation. More precisely, the non-linear interdependence is quantified by the Phase Locking Value  $\zeta_{n,m}$  [3], which casts a locking unitary value of  $n$  cycles from one oscillation to  $m$  cycles of the other. The  $n,m$  values are chosen based on the central frequencies relations for each pair of power bands. This method engages a couple of convolutions between the EEG or HRV filtered signal and the complex-valued Gabor wavelet [6]. Then, the differences of instantaneous phases  $\hat{\phi}_{n,m}[k]$  are computed at each time instant, which in turn, are mapped to a cyclic  $[0, 2\pi m)$  interval. And, the strength of the interdependence is quantified by the magnitude of the phases differences expectation  $E\{\cdot\}$ ; such a measure is known as PLV, as Eq. 2 denotes.

$$\zeta_{n,m} = \sqrt{(E\{\cos \hat{\phi}_{n,m}[k]\})^2 + (E\{\sin \hat{\phi}_{n,m}[k]\})^2} \quad (2)$$

To finalise, a normalisation routine is applied to fit the generated features into 0 – 1 interval, to improve the results interpretation of further statistical analyses.

### D. Statistical analysis

By dealing with biological signals, an evaluation of Gaussian conditions is required, in order to conduct an appropriate statistical analysis beneath the clinical cohort. The Bartlett test assessed an analytical divergence of the mean and covariance of the modelled data versus the Gaussian distribution. Those preliminary inspections proved a strong deviation from the Gaussian tendency, suggesting the application of a series of Kruskal-Wallis rank tests [11]. Such an omnibus test lacks of the ability to differentiate the inter-neural cluster casting the significant difference, but its corresponding coupling/decoupling activity intends to elicit interactions with significant values  $p < 0.05$  amongst bands and sleep stages.

## III. RESULTS

The linear analysis represented by the wavelet coherence, arranged one sleep cycle into a multi-stage periodogram, which included EEG/HRV power bands and averaged out clinical group. Out of the macro-periodogram in Fig. 1, the coherence between low-regime EEG bands, such as  $\delta, \theta \leftrightarrow$  LF, HF was turning stronger (0.4 – 0.5) over W and REM stages. Inasmuch as, we moved to  $\theta, \sigma$  and  $\beta$  oscillations in relation to HF, it was observed an increasing activity (0.5 – 0.7) in deep sleep stages, S3 and S4. Opposite to this, EEG  $\leftrightarrow$  LF relationship hardly exceeded 0.4 – 0.45 coherence levels. One of the most interesting matters was the

TABLE I  
INTER-NEURAL CLUSTERS

Parcel	Electrodes	Abbreviation
1	$C_3A_2, C_zA_1, C_4A_1$	$C_{4:3}$
2	$O_2A_1, O_1A_2$	$O_{21}$
3	$F_8A_1, F_7A_2$	$F_{87}$
4	$F_4A_1, F_3A_2$	$F_{43}$
5	$P_4P_3, P_4P_2, P_3P_2$	$P_{43}$
6	$T_3T_5, T_4T_6$	$T_{43}$

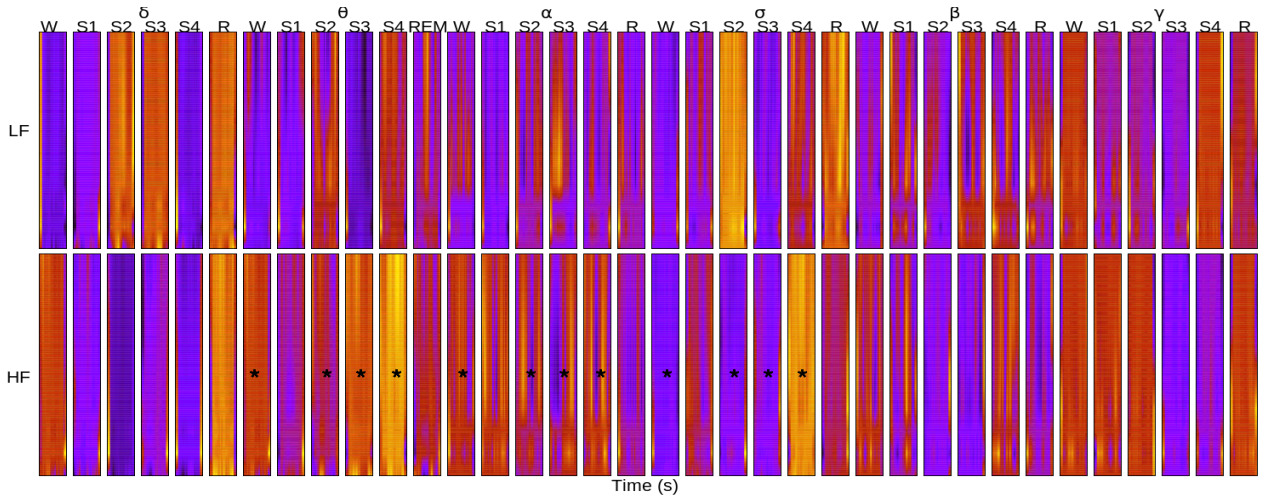


Fig. 1. Macro-periodiogram of Wavelet Coherence considering EEG  $\delta$ ,  $\theta$ ,  $\alpha$ ,  $\sigma$ ,  $\beta$  and  $\gamma$  at  $C_{4z3}$  parcel against HRV LF and HF bands for sleep stages W, S1, S2, S3, S4 and REM. On the x-axis, each periodogram's cell portrays averaged out 30-seconds epochs corresponding to a particular sleep stage over the 10 subjects, and 12 wavelet-scaled pseudo-frequencies are ordered on the y-axis starting on *ca.* 89.8 Hz till (top scale) 0.04 Hz (bottom scale). The colour scale assigns the black-violet spectrum for low coherence values, whilst red-yellow intensities represent the surrounding unitary values, i.e. high coherence. \* statistically significant ( $p < 0.05$ ) after Kruskal-Wallis rank test.

uniform coherence between  $\theta \leftrightarrow$  HF bands along the 6 sleep stages, which slowly faded out to mid-level coherence (0.5) from  $\sigma$  band region. In respect to the remaining inter-neural clusters, which are not shown here; it was corroborated the bright activity (0.6 – 0.75) of EEG low-regime bands  $\delta/\theta \leftrightarrow$  LF/HF, moving towards dissipating levels at  $\alpha$  to  $\gamma$  frequencies.

In correspondence to the non-linear analysis,  $n:m$  phase synchronisation realised polar diagrams to illustrate the cross-frequency locking values at each sleep stage. The functional interdependence in EEG  $\leftrightarrow$  HF power bands maintained a regular mid-value (0.3 – 0.4) for W, S1 and REM stages. Focusing on low-regime bands  $\delta$  and  $\theta$ , the S4 reached its highest value around 0.6. As far as we moved to  $\alpha$  band, S3 took the lead, and finally S2 consolidated the strongest phase interaction within  $\sigma$  and  $\beta$  bands. Due to the lack of statistically significant results and space limitations, the polar diagrams for this case are not displayed. On the contrary, EEG  $\leftrightarrow$  LF interactions in Fig. 2 showed that S4 and REM stages surpassed 0.6 locking level at both extremes of the neuronal spectrum, i.e.  $\delta$  and  $\beta$  power bands. Similarly, S1 stage registered a noticeable deviation (0.7), when  $\sigma$  oscillation was concerned. For the remaining power bands and sleep stages, the synchronisation strength preserved homogeneous values around 0.4. None radical difference was found in the polar diagrams of the alternative inter-neural clusters.

Lastly, a series of omnibus Kruskal-Wallis rank tests were addressed in order to identify significant differences, attending to all interactions of EEG  $\leftrightarrow$  HRV power bands, sleep stages and electrode clusters. Wavelet coherence (WCOH) method elicited a larger number of significant values including W, light (S2) and deep sleep (S3, S4) stages between  $\theta$ ,  $\alpha$ ,  $\sigma \leftrightarrow$  HF frequency pairs with ( $\chi^2 = 11.76, p = 0.038$ ) and ( $\chi^2 = 13.11, p = 0.022$ ) test values. Nonetheless, no

significant results turned to be sufficiently divergent between neuronal EEG bands and HRV-LF by the time of wavelet coherence evaluation. In contrast, PLV did reveal relevant differences between  $\theta$  ( $\chi^2 = 11.76, p = 0.038$ ),  $\alpha$  ( $\chi^2 = 13.11, p = 0.022$ ),  $\sigma$  ( $\chi^2 = 11.76, p = 0.038$ ) and HRV-LF cross-frequencies, located at S2 and REM stages. Figures 1 and 2 labelled the statistically significant values (using \*) according to these criteria.

#### IV. DISCUSSION AND CONCLUSIONS

The predominant activity of LF cardiac band during W/REM stages, as well as, HF along NREM periods have been claimed by previous works [12]. Our findings not only reaffirmed that statement, but also evidenced the coherence related to the low-regime EEG frequency bands, i.e. W and REM stages kept a coherent interdependence with sympathetic system (HRV LF). Beside this, a progressive retreat of cross-frequency interaction was detected during NREM stages, which is explained by a vagal cardiac system emergence or HF power band ascendancy. A novel issue of this work suggested the strong interdependence of  $\delta$  and  $\theta$  oscillations, in contrast to the weak interactions of the high-regime power bands, such as  $\beta$  and  $\gamma$ . Consequently, we sustain that the functional interdependencies of sympathetic and parasympathetic are vaguely related to high neuronal oscillations within healthy population.

Wavelet coherence and PLV coincided on the interdependence of the sympathetic system (HRV LF) across W and REM stages. Furthermore, it was demonstrated from a non-linear approach, the intrinsic phase-coupled activity of parasympathetic system (HRV HF) during NREM episodes. Although,  $n:m$  phase synchronisation is strictly constrained to the choice of non-arbitrary pairs of central frequencies, whereas it can only exist a rational quotient in between. In this manner, we can assure that  $n, m$  integers are invariant

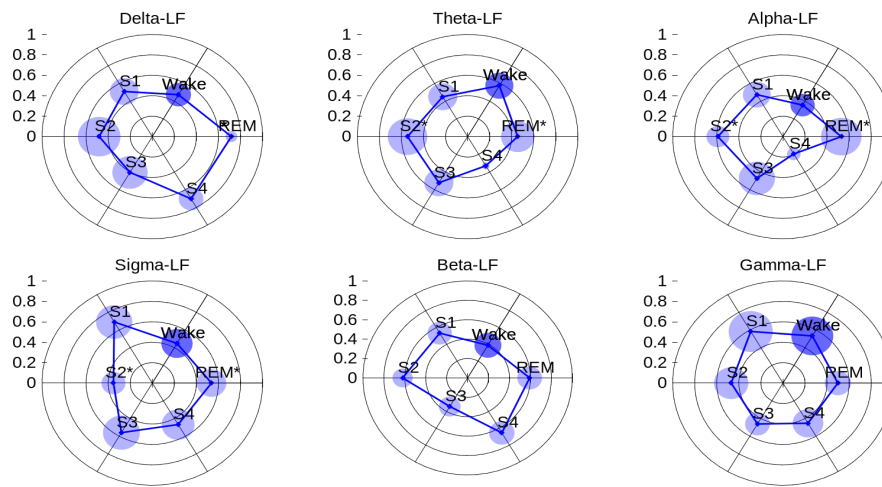


Fig. 2. Polar diagram of  $n:m$  Phase Synchronisation for clinical cohort. Phase Locking Value between  $C_{4\pm 3}-\delta$ ,  $\theta$ ,  $\alpha$ ,  $\sigma$ ,  $\beta$  and  $\gamma$  versus HRV LF band. The coloured point represent the absolute mean PLV between 0-to-1 scale at each sleep stage, accompanied by a centred circle expressing the standard deviation amongst the group members. \* statistically significant ( $p < 0.05$ ) after Kruskal-Wallis rank test.

to multiples of phase slips [13]. Even though this condition holds, larger  $n$ ,  $m$  integer values could produce unstable and less robust synchronisations, e.g. spurious couplings, due to the implicit commutative variance.

From the results of Kruskal-Wallis rank tests, we could statistically confirm most of the conclusions here previously suggested. First, wavelet coherence method highlighted the statistically importance of interactions at  $\theta$ ,  $\alpha$  and  $\sigma$  power bands, but only related to the vagal cardiac (parasympathetic) activity during NREM sleep stages (W, S2, S3, S4). However, PLV became a suitable complement to describe neuronal and sympathetic activity, which involved the same power bands, but limited to S2 and REM stages. Such findings concurred with previous studies [14] [12] with the novel corroboration of associated linear and non-linear approaches. Although, further data analyses should be conducted, in order to discard eventual overestimations misleading these findings. Until now, we can hypothesise that TFA-based methods are more reliable to discriminate functional interdependencies within parasympathetic system. Foremost, PLV estimated in a more accurate way the strong interaction of  $\theta$ ,  $\alpha$  and  $\sigma$  bands to differentiate the sympathetic counterpart.

The obtained results indicate the existence of significant differences between EEG and HRV power bands, in terms of time-frequency coherence and phase synchronisation across overnight sleep cycles. Moreover, the influence between mid-range EEG bands and parasympathetic activity during light and deep sleep stages was enhanced by the tracking of functional interdependencies during W stage. It is advised, the conduction of additional studies to determine with more detail the impact of non-linear approaches, e.g. surrogate data analysis. In consonance, TFA-oriented approaches for the differentiation of sleep physiopathologies, should be more extensively explored.

## REFERENCES

- [1] M. Dumont, F. Jurysta, J.-P. Lanquart, P.-F. Migeotte, P. van de Borne, and P. Linkowski, "Interdependency between heart rate variability and sleep EEG: linear/non-linear?" *Clinical Neurophysiology*, vol. 115, no. 9, pp. 2031 – 2040, 2004.
- [2] U. R. Acharya, K. P. Joseph, N. Kannathal, C. M. Lim, and J. S. Suri, "Heart rate variability: A review." *Medical & Biological Engineering & Computing*, vol. 44, no. 12, pp. 1031 – 1051, 2006.
- [3] J. Palva, S. Palva, and K. Kaila, "Phase synchrony among neuronal oscillations in the human cortex," *Journal of Neuroscience*, vol. 25, no. 15, pp. 3962–3972, April 2005.
- [4] R. Bartsch, J. W. Kantelhardt, T. Penzel, and S. Havlin, "Experimental evidence for phase synchronization transitions in the human cardiorespiratory system," *Phys. Rev. Lett.*, vol. 98, p. 054102, Feb 2007.
- [5] S. Dimitriadis, N. Laskaris, Y. Del Rio-Portilla, and G. Koudounis, "Characterizing dynamic functional connectivity across sleep stages from EEG," *Brain Topography*, vol. 22, no. 2, pp. 119–133, 2009, cited By (since 1996) 13.
- [6] K. Mezeiova and M. Palus, "Comparison of coherence and phase synchronization of the human sleep electroencephalogram," *Clinical Neurophysiology*, vol. 123, no. 9, pp. 1821 – 1830, 2012.
- [7] S. Palva, S. Monto, and J. M. Palva, "Graph properties of synchronized cortical networks during visual working memory maintenance," *NeuroImage*, vol. 49, no. 4, pp. 3257 – 3268, 2010.
- [8] E. Pereda, R. Q. Quiroga, and J. Bhattacharya, "Nonlinear multivariate analysis of neurophysiological signals," *Progress in Neurobiology*, vol. 77, no. 12, pp. 1 – 37, 2005.
- [9] T. F. of The European Society of Cardiology, T. N. A. S. of Pacing, and Electrophysiology, "Heart rate variability," *European Heart Journal*, vol. 17, pp. 354–381, 1996.
- [10] S. Mallat, *A Wavelet Tour of Signal Processing*. Elsevier Academic Press, 1999.
- [11] D. Chicharro and R. G. Andrzejak, "Reliable detection of directional couplings using rank statistics," *Phys. Rev. E*, vol. 80, p. 026217, Aug 2009.
- [12] F. Jurysta, J.-P. Lanquart, V. Sputaels, M. Dumont, P.-F. Migeotte, S. Leistedt, P. Linkowski, and P. van de Borne, "The impact of chronic primary insomnia on the heart rate EEG variability link," *Clinical Neurophysiology*, vol. 120, no. 6, pp. 1054 – 1060, 2009.
- [13] M. Wacker and H. Witte, "On the stability of the  $n:m$  phase synchronization index," *Biomedical Engineering, IEEE Transactions on*, vol. 58, no. 2, pp. 332–338, 2011.
- [14] M. Dumont, F. Jurysta, J.-P. Lanquart, A. Nosedá, P. van de Borne, and P. Linkowski, "Scale-free dynamics of the synchronization between sleep EEG power bands and the high frequency component of heart rate variability in normal men and patients with sleep apnea hypopnea syndrome," *Clinical Neurophysiology*, vol. 118, no. 12, pp. 2752 – 2764, 2007.